

## Magnetic Barkhausen Noise Analysis for Microstructural Effects Separation during Flow Forming of Metastable Austenite 304L

Julian ROZO VASQUEZ <sup>1</sup>, Bahman ARIAN <sup>2</sup>, Markus RIEPOLD <sup>3</sup>  
Werner HOMBERG <sup>2</sup>, Ansgar TRÄCHTLER <sup>3</sup>, Frank WALTHER <sup>1</sup>

<sup>1</sup> Chair of Materials Test Engineering (WPT), TU Dortmund University, Dortmund, NRW, Germany;  
Phone: +49 231 755-8535, Fax: +49 231 755-8029; e-mail: julian.rozo@tu-dortmund.de; frank.walther@tu-dortmund.de

<sup>2</sup> Chair of Forming and Machining Technology (LUF), Paderborn University, Paderborn, NRW, Germany;  
e-mail: ba@luf.uni-paderborn.de; wh@luf.uni-paderborn.de

<sup>3</sup> Fraunhofer Institute for Mechatronic System Design (IEM), Paderborn, NRW, Germany;  
e-mail: markus.riepold@iem.fraunhofer.de; ansgar.traechtler@iem.fraunhofer.de

### Abstract

This work deals with the analysis of the influence of different microstructural effects on non-destructive micromagnetic testing using magnetic Barkhausen noise (MBN) analysis, during flow forming of austenitic steel 304L tubes. This is necessary for the implementation of non-destructive MBN testing within the model of a soft sensor for closed-loop control systems. A characterization of the specimens was carried out by means of  $\alpha'$ -martensite measurements, hardness tests, residual stresses and surface roughness. The aim is to establish the influence of the different microstructural effects on the measured MBN parameter, the maximum MBN amplitude  $M_{\max}$ . The strain-induced hardening, evolution of residual stresses and phase transformation during plastic deformation have a direct influence in the development of the  $M_{\max}$  parameter. However, a lower surface roughness triggers a mitigating effect on the MBN signals. This information is valuable to define the operation window of the sensor within the material modeling for property control.

**Keywords:** Magnetic Barkhausen noise, microstructural effect separation, ferromagnetic phase,  $\alpha'$ -martensite, flow forming, metastable austenitic steel, soft sensor, closed-loop control

## 1. Introduction

The implementation of control engineering within metal forming processes has gained recently relevance in the production of high quality components with optimized properties in industries like automotive and aeronautics. Metastable austenitic stainless steels have been used in these applications thanks to their high strength, corrosion resistance and good formability. During plastic deformation of these steels, strain-induced phase transformation of non-magnetic austenite into ferromagnetic  $\alpha'$ -martensite occurs [1]. This phase transformation can be measured by means of the change of magnetic properties using the non-destructive magnetic Barkhausen noise (MBN) effect [2,3]. Non-destructive testing plays a key role in the implementation of control engineering in production systems, since the measured parameters can be used as control variables of the closed-loop control systems.

In this work, non-destructive testing, specifically MBN analysis, has been used to monitor the strain hardening and phase transformation during flow forming of austenitic steel AISI 304L. This entails the formulation of correlations between the measured MBN parameters and different microstructural phenomena that occur during manufacturing processes. Many studies describe correlations between MBN testing and hardening [4], residual stresses [5], surface condition [6,7] and phase transformation [2,8], that occur during plastic deformation of steels. Since the MBN measurements contain the effects



of the mentioned phenomena, the identification of their influence is crucial to model the material behaviour. The focus of this work is the assessment of the influence of those factors on the measured MBN signals on flow formed components. This is helpful to define the operation window of the micromagnetic sensor in the frame of the soft sensor design for closed-loop property control.

## 2. Materials and Methods

### 2.1. Specimens

The specimens were manufactured using seamless tubes made of stainless steel AISI 304L (X2CrNi18-9, 1.4307) with 80 mm outer diameter and 4 mm wall thickness. The production was carried out by means of the flow forming machine BD 40 (Bohner & Koehle GmbH & Co. KG, Esslingen, Germany) (Figure 1a) at the LUF. The specimens were manufactured at room temperature, with a rotation speed of  $s = 30$  rpm and using feed rates between  $f = 6$  and 60 mm/min. The focus will be on the specimens produced with feed rates of 6 mm/min (specimen 1) and 60 mm/min (specimen 2). The flow forming operation was performed using three rollers to reduce the wall thickness of the tubes. The initial 4 mm wall thickness was reduced by 1 mm in each flow forming step. Starting from the initial condition “IC” (metastable austenite), different forming operations were performed to produce three forming zones (FZ 1, 2 and 3) (Figure 1b). Each forming zone corresponds to a plastic deformation state with a defined amount of strain-induced  $\alpha'$ -martensite. The final workpieces manufactured during the production process are shown in Figure 1c.

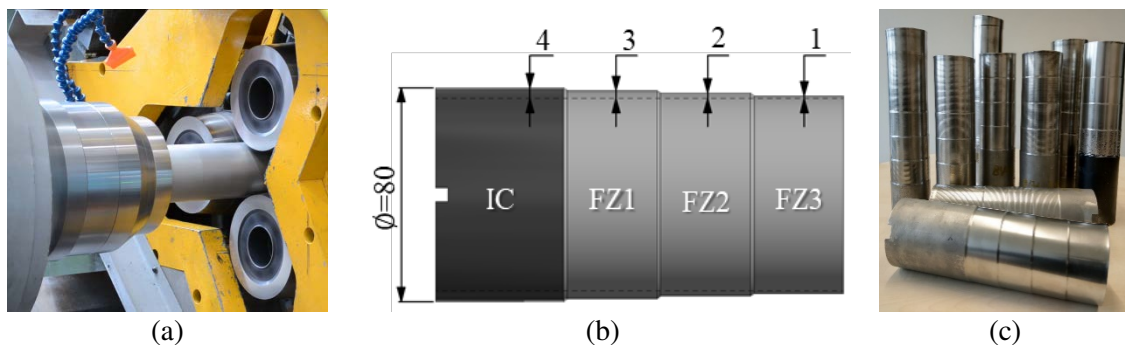


Figure 1. Specimen manufacture: (a) Flow forming machine; (b) geometry and dimensions (in mm), (c) final workpieces.

### 2.2. Measurements of surface roughness and microscopic inspection of the surface condition

The roughness of the initial condition and the different forming zones of the specimens 1 and 2 were measured by means of the tactile device MarSurf M300 (Mahr GmbH, Goettingen, Germany) (Figure 2a). The values of the arithmetic mean roughness ( $R_a$ ) and the mean peak-to-valley height ( $R_z$ ) of the outer surface of the specimens were measured. The data was obtained locating the probe tip normal to the curved outer surface of the specimens, using the corresponding prisms (Figure 2a).

In order to obtain graphical information of the surface condition, an inspection was performed using the digital microscope Keyence VHX-500F (Keyence Corp., Osaka, Japan) (Figure 2b).



Figure 2. (a) Roughness measurements with the MarSurf M300 and (b) microscopic inspection of the surface with the Keyence VHX-500F.

### 2.3. Analysis of residual stress by means of X-ray diffraction (XRD)

The residual stresses were determined by means of the analysis of X-ray diffraction of the outer surface of the specimens. The measurements were carried out using the X-ray diffractor Bruker D8 Discover (Bruker Corp., Billerica, Massachusetts, USA) with a 1 mm collimator. The analysis of residual stresses for the austenitic phase (IC) was performed at  $2\theta = 95.989^\circ$ , which corresponds to the Miller index  $\{h\ k\ l\} = \{2\ 2\ 2\}$ . Similarly, the analyses of the martensitic phase (FZ1 to 3) were carried out at  $2\theta = 82.329^\circ$  in the plane  $\{h\ k\ l\} = \{2\ 1\ 1\}$ . The data to perform X-ray diffraction analyses regarding the mentioned  $2\theta$  angles were extracted from the report by Eigenmann et al. [9].

### 2.4. Measurements of $\alpha'$ -martensite content

Measurements of the  $\alpha'$ -martensite content close to the outer surface of the tubes were carried out by means of the Feritscope FMP30 (Helmut Fischer GmbH, Sindelfingen, Germany). This device works under the magneto-inductive principle to measure the ferritic phase content. By means of the correlations developed by Talonen et al., 2004, the  $\alpha'$ -martensite contents can be determined from the ferritic phase measurements [8]. However, these measurements cannot be used in closed-loop control systems, because the online acquisition and transmission of the data is not possible during the production process. For this reason, the use of micromagnetic testing is a convenient alternative as soft sensor for the property control.

### 2.5. Micromagnetic testing by means of the 3MA-II system

Micromagnetic analyses are based on the behavior of ferromagnetic materials, such as metastable austenitic steel AISI 304L. In ferromagnetic materials, the magnetic induction  $B$ , triggered by a magnetic field  $H$ , can be described by means of the magnetization hysteresis (Figure 3a). These materials are divided by means of Bloch walls in spontaneously magnetized regions, called magnetic domains. During magnetization and demagnetization of the material, the walls move in response to the applied field. This motion is jerky and discontinuous, producing the Barkhausen effect, that can be evidenced in the magnetization hysteresis at high scale. This effect is influenced by the interaction of the walls with lattice defects, dislocations, phase changes, grain boundaries and residual stresses. This way, from the

magnetic Barkhausen noise (MBN) curve (Figure 3a), the maximum amplitude of the MBN profile ( $M_{max}$ ) is the parameter of interest [10–12].

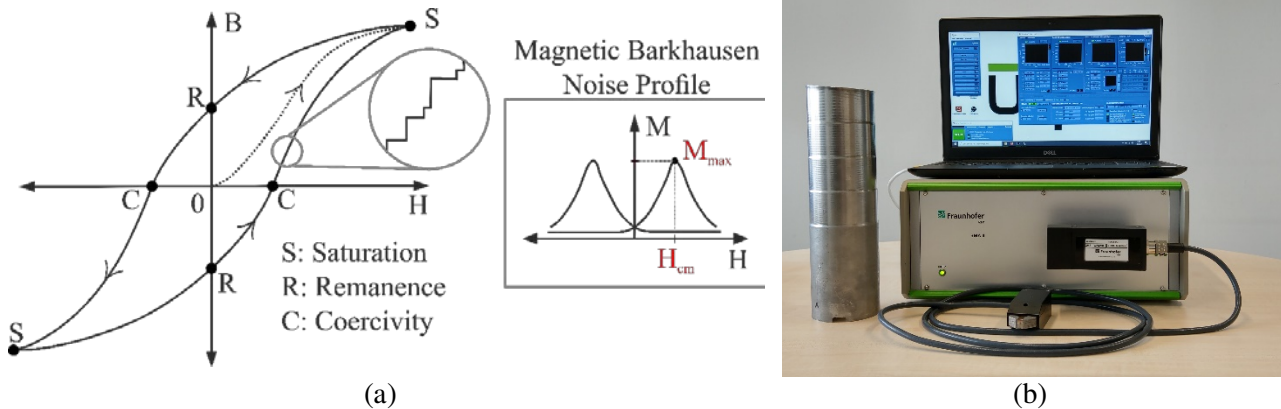


Figure 3. Micromagnetic testing: (a) Hysteresis loop and MBN profile; (b) 3MA-II system device and flow-formed specimen.

In this work, the micromagnetic measurements were carried out using the 3MA-II system (Fraunhofer IZFP, Saarbruecken, Germany), with the sensor SN18201 in contact with the outer surface of the specimens (Figure 3b).

### 3. Results and Discussions

#### 3.1. Surface condition inspection and roughness measurements

An inspection of the surface of both specimens were performed with the digital microscope Keyence VHX-500F. The results reported in Figure 4 correspond to the forming zone 2 (FZ2) of both specimens. The upper pictures correspond to a 30x magnification and the lower to 100x. No remarkable difference of the surface condition was evidenced on the different forming zones of the same specimen. A qualitative analysis of the results evidences a higher degree of surface damage in the specimen produced with a feed rate  $f = 60$  mm/min (specimen 2). For a constant rotation speed  $s = 30$  rpm of the workpiece, the higher the feed rate of the roller tools, the lower the contact time with the outer surface of the specimen. This entails a less uniform plastic deformation evidenced in lower surface quality.

A quantitative validation of this inspection was carried out by means of roughness measurements. The results for specimens 1 and 2 and their respective forming zones are summarized in Table 1. The measurements were performed as described in section 2.2 using the tactile device MarSurf M300. The roughness values of the initial condition in both specimens are similar, with values around  $R_a = 1.33$   $\mu\text{m}$ . The mean roughness values of the specimens produced with 6 mm/min (specimen 1) are 90% lower than those for specimens produced with 60 mm/min (specimen 2). Since the rotation speed remains constant, the contact time between the roller tools and the workpieces is higher at lower feed rates, as a result the plastic deformation is more uniform.

The roughness values of the different forming zones (FZ1 to FZ3) within the same specimen show a decreasing behaviour. A higher number of overruns is required to achieve FZ3 compared to FZ1. This entails a higher contact time between the roller tools and the workpiece, therefore a more uniform plastic deformation is evidenced in zones with higher number of overruns. An analysis of the data for specimen 2 shows that the best roughness value (in FZ3) is higher than the roughness of the initial condition, which is undesired concerning the surface quality of the components. This allows the definition of process windows regarding the parameters for production of optimized components.

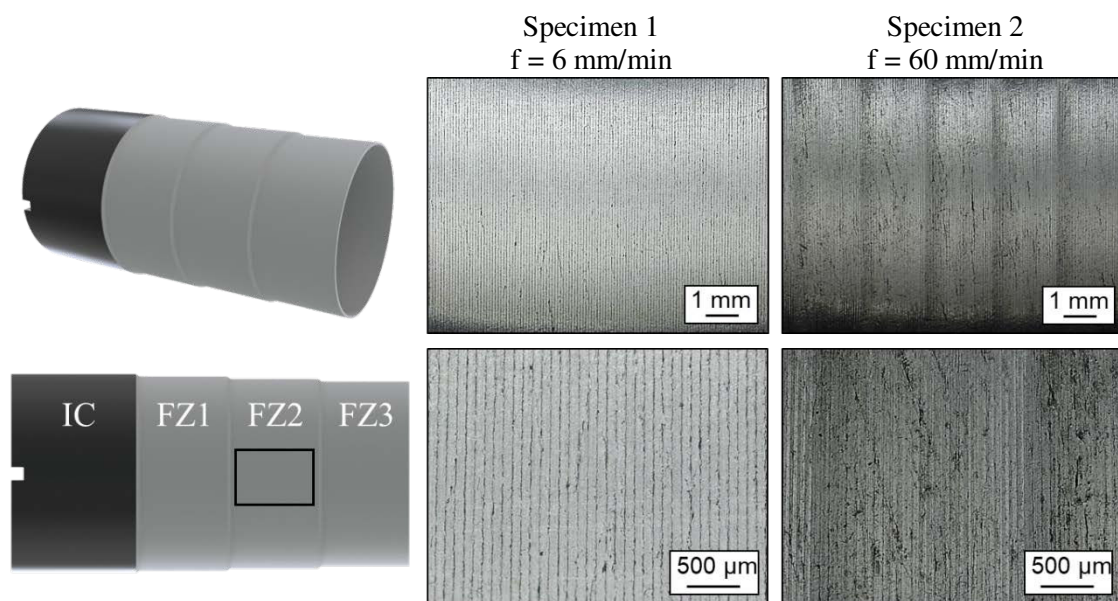


Figure 4. Microscopic investigation of the surface condition of specimens produced using different feed rates.

**Table 1. Results of surface roughness measurements for the different forming zones of specimens produced with two different feed rates**

Specimen	Forming zone	Surface roughness	
		Arithmetic mean roughness, Ra [ $\mu\text{m}$ ]	Mean peak-to-valley height, Rz [ $\mu\text{m}$ ]
Specimen 1 f = 6 mm/min	IC	1.33	10.03
	FZ1	0.321	2.599
	FZ2	0.343	3.318
	FZ3	0.249	1.718
Specimen 2 f = 60 mm/min	IC	1.38	10.5
	FZ1	3.47	13.63
	FZ2	2.449	11.76
	FZ3	1.961	8.555

The values of surface roughness of both specimens on the different forming zones were plotted in Figure 5 to identify their influence in the non-destructive testing by means of the micromagnetic analysis.

### 3.2. Residual stresses

The residual stresses of the outer surface of the flow formed specimens were measured according to the specifications described in section 2.3. The results (Table 2) show that the workpieces have compressive residual stresses in the initial condition and the different forming zones. At the initial condition the measured residual stresses were around -547.5 MPa. The plastic deformation in both specimens causes an increment of the residual stresses, reaching a maximum about -220 MPa. The successive plastic deformation on FZ 2 and 3, increases the compressive residual stresses to obtain values -374.3 MPa for specimen 1 and -326.4 MPa for specimen 2. It is well known that compressive residual stresses induced by means of manufacturing processes like turning and in this case metal forming, increase fatigue life, corrosion and wear resistance [13]. This entails a positive effect of the flow forming of tubes for their final uses.

**Table 2. Results of residual stresses for the different forming zones of specimens produced with two different feed rates**

Specimen	Forming zone	Residual stress, RS [MPa]
Specimen 1 f = 6 mm/min	IC	-547.5
	FZ1	-229.8
	FZ2	-365.1
	FZ3	-374.3
Specimen 2 f = 60 mm/min	IC	-547.5
	FZ1	-220.1
	FZ2	-285
	FZ3	-326.4

The values of residual stresses were plotted in Figure 5 to analyse their effect in the non-destructive micromagnetic testing.

### 3.3. Separation of effects during non-destructive testing by means of micromagnetic analysis

Figure 5 shows the correlation of the non-destructive micromagnetic testing by means of the magnetic Barkhausen noise (MBN) analysis with other characterization techniques. The graphics show the evolution of different microstructural phenomena that occur during flow forming of austenitic stainless steel 304L. The strain-induced phase transformation during plastic deformation is shown by means of the  $\alpha'$ -martensite content. The microstructural mechanisms of phase transformation during flow forming were discussed by the authors in [14]. The higher the thickness reduction, the higher the  $\alpha'$ -martensite volume. The strain-induced hardening is well correlated with the phase transformation. Likewise, the maximum amplitude of the MBN profile ( $M_{max}$ ) grows consequently with the evolution of  $\alpha'$ -martensite volume and the hardness, as it was evidenced in previous investigations [2,15]. This parameter is even sensible to the saturation at the final states of deformation (FZ2 and 3) for the specimen 1, as can be evidenced in the plateau of the curves.

A comparison of the  $\alpha'$ -martensite volume and the hardness in both specimens leads to the conclusion that specimens produced with lower feed rates, undergo a faster saturation and higher values of  $\alpha'$ -

martensite. This is related to the discussion on section 3.1 regarding the uniformity of plastic deformation depending on the feed rate parameter. As discussed in section 2.5, the MBN analysis contains a mixture of different microstructural effects that occur during plastic deformation like phase transformation, grain boundaries, residual stresses and surface damage, evaluated here by means of surface roughness. The transition from the non-magnetic austenite to the ferromagnetic martensitic phase is the predominant effect influencing the growth of  $M_{max}$  with the deformation. This phase transformation entails a microstructural change in the grain size, which increases the amount of grain boundaries and consequently the number of pinning sites of the magnetic domains [2,10]. For this reason, higher MBN values correspond to higher deformation states, according to the references [16,17]. As it was described in section 3.2, the compressive residual stresses in the martensitic phase (FZ1 to 3) increase with the deformation. This entails an increment of  $M_{max}$ , which is consistent with previous investigations [5,18].

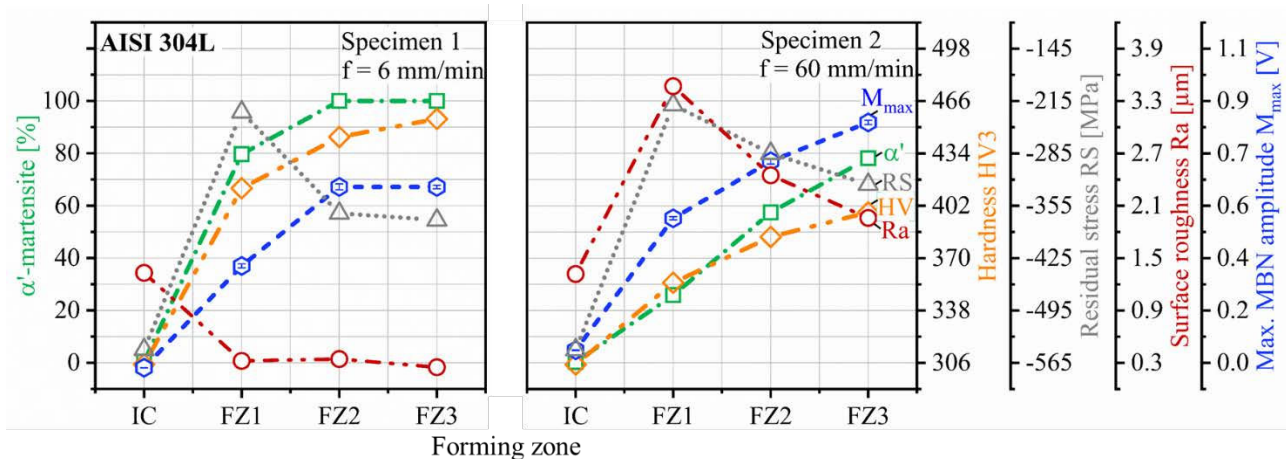


Figure 5. Results of the correlations between non-destructive testing by means of MBN and microstructural phenomena like hardening, residual stresses and roughness, during plastic deformation of austenitic steel AISI 304L.

However, one controversial aspect arises from the fact that the  $M_{max}$  curve of the specimen 1 develops below to the corresponding curve of the specimen 2. Despite higher  $\alpha'$ -martensite content in specimen 1 in all deformed states (FZ1 to FZ3), the measured  $M_{max}$  parameter is always higher for the specimen 2. An analysis of the data in Figure 5 allows to conclude that the good surface condition of specimen 1 after plastic deformation has an attenuating effect on the micromagnetic measurements performed with 3MA-II System. This result is consistent with previous studies that prove the suitability of the non-destructive micromagnetic testing to characterize wear and surface damage. In those investigations the more wear the surfaces have, the higher the measured  $M_{max}$  values [6,19].

This information is valuable to define the operation window of the micromagnetic sensor for property control. The soft sensor model to define the  $\alpha'$ -martensite content in terms of the variable  $M_{max}$ , should consider the remarkable influence of the surface condition of the workpieces on the micromagnetic measurements.

### 3. Conclusions and outlook

In this work, an assessment of the influence of different microstructural phenomena on non-destructive micromagnetic testing by means of magnetic Barkhausen noise (MBN) analysis was successfully carried out. The information obtained is valuable to define the operation window of the micromagnetic sensor in a closed-loop property control during flow forming of austenitic stainless steel tubes. Plastic deformation of this material triggers residual stresses, strain-induced hardening and phase transformation, specifically from metastable austenite into  $\alpha'$ -martensite. It was proved that the MBN testing can be used to monitor the microstructural evolution of the specimens during deformation, because there is a direct correlation between the measured MBN signals and the content of the ferromagnetic phase  $\alpha'$ -martensite. Consequently, the increment of compressive residual stresses matches with the incremental behavior of the micromagnetic parameters. However, it was evidenced that the quality of the tested surfaces plays a key role in the evolution of the MBN signals. A better surface quality causes an attenuation of the micromagnetic measurements. As the surface quality depends on process parameters like feed rate, a comprehensive assessment of the connection between process parameters and component properties was carried out. This means a step forward in the soft sensor model for a closed-loop property control.

Future work will focus on the implementation of these results within the material model of the soft sensor for property control. This entails a quantitative assessment of the surface condition effect on micromagnetic testing. With this information, an improvement of the soft sensor is possible, since the operation process window of the micromagnetic sensor will be related to the process parameters and the final goal to produce high quality products with optimized properties.

### Acknowledgements

The authors would like to thank the German Research Foundation (Deutsche Forschungsgemeinschaft, DFG) for the support of the depicted research within the priority program SPP 2183 “Property Controlled Deformation Processes”, through project No. 424335026 “Property Control During Spinning of Metastable Austenites”.

### References

- [1] P. Haušild; K. Kolařík; M. Karlík, 'Characterization of strain-induced martensitic transformation in A301 stainless steel by Barkhausen noise measurement', *Materials & Design*, Vol 44, pp 548–554, 2013.
- [2] M. Astudillo; M. Nicolás; J. Ruzzante; M. Gómez; G. Ferrari; L. Padovese; M. Pumarega, 'Correlation between martensitic phase transformation and magnetic Barkhausen noise of AISI 304 steel', *Procedia Mater. Sci.*, Vol 9, pp 435–443, 2015.
- [3] J. Anglada-Rivera; L. Padovese; J. Capó-Sánchez, 'Magnetic Barkhausen Noise and hysteresis loop in commercial carbon steel: Influence of applied tensile stress and grain size', *J. Magn. Mater.*, Vol 231, pp 299–306, 2001.
- [4] M. Neyra Astudillo; N. Núñez; M. López Pumarega; J. Ruzzante; L. Padovese, 'Magnetic Barkhausen noise and magneto acoustic emission in stainless steel plates', *Procedia Mater. Sci.*, Vol 8, pp 674–682, 2015.

- [5] S. Schuster; L. Dertinger; D. Dapprich; J. Gibmeier, 'Application of magnetic Barkhausen noise for residual stress analysis – Consideration of the microstructure', *Mater. Test.*, Vol 60, No 6, pp 545–552, 2018.
- [6] L. Samfaß; N. Baak; R. Meya; O. Hering; A. Tekkaya; F. Walther, 'Micro-magnetic damage characterization of bent and cold forged parts', *Prod. Eng.*, Vol 14, No 1, pp 77–85, 2020.
- [7] M. Teschke; J. Rozo Vasquez; L. Lücker; F. Walther, 'Characterization of damage evolution on hot flat rolled mild steel sheets by means of micromagnetic parameters and fatigue strength determination', *Materials*, Vol 13, No 11, 2020.
- [8] J. Talonen; P. Aspegren; H. Hänninen, 'Comparison of different methods for measuring strain induced  $\alpha$ -martensite content in austenitic steels', *Mater. Sci. and Tech.*, Vol 20, No 12, pp 1506–1512, 2004.
- [9] B. Eigenmann; E. Macherauch, 'Röntgenographische Untersuchung von Spannungszuständen in Werkstoffen. Teil III', *Matwiss. Werkstofftech.*, Vol 27, No 9, pp 426–437, 1996.
- [10] D. Jiles, 'Introduction to magnetism and magnetic materials. Chapman & Hall, London, 1991, ISBN 978-0-412-38640-4.
- [11] B. Cullity; C. Graham, 'Introduction to magnetic materials. IEEE/Wiley, Hoboken N.J., 2009.
- [12] S. Chikazumi, 'Physics of magnetism. John Wiley & Sons, Inc., New York, NY, USA., 1966.
- [13] Edoardo Capello, 'Residual stresses in turning: Part I: Influence of process parameters', *J. Mat. Proc. Tech.*, Vol 160, No 2, pp 221–228, 2005.
- [14] J. Rozo Vasquez; B. Arian; M. Riepold; W. Homberg; A. Trächtler; F. Walther, 'Microstructural investigation on phase transformation during flow forming of the metastable austenite AISI 304. In: Neidel, A. (Hrsg.) - Fortschritte in der Metallographie- Sonderbände der Praktischen Metallographie zur 54. Metallographie-Tagung, 75–81, Saarbruecken, Germany, 2020.
- [15] M. Neslušan; J. Šugárová; P. Haušild; P. Minárik; J. Čapek; M. Jambor; P. Šugár, 'Barkhausen noise emission in AISI 321 austenitic steel originating from the strain-induced martensite transformation', *Metals*, Vol 11, No 3, pp 429, 2021.
- [16] S. Yamaura; Y. Furuya; T. Watanabe, 'The effect of grain boundary microstructure on Barkhausen noise in ferromagnetic materials', *Acta Mater.*, Vol 49, pp 3019–3027, 2001.
- [17] Z. Wang; Y. Gu; Y. Wang, 'A review of three magnetic NDT technologies', *J. Magn. Mater.*, Vol 324, No 4, pp 382–388, 2012.
- [18] F. Eichhorn; M. Zschau, 'Messung des Eigenspannungsabbaus durch Analyse des Barkhausen-Rauschens', *Z. Werkstofftech.*, Vol 11, pp 213–216, 1980.
- [19] J. Tenkamp; M. Haack; F. Walther; M. Weibring; P. Tenberge, 'Application of micro-magnetic testing systems for non-destructive analysis of wear progress in case-hardened 16MnCr5', *Mater. Test.*, Vol 58, No 9, pp 709–716, 2016.